International Research Journal of Engineering and Technology (IRJET) e-ISSN: 2395-0056
Volume: 05 Issue: 02 | Feb-2018 www.irjet.net p-ISSN: 2395-0072

# Numerical Investigation on Effect of Geometrical Variations in Microchannel Heat Sink

**Sharad D. Patil[1], Sagar C. Wangdare[2]**

[1,2] *Department of Mechanical Engineering, Rajarambapu Institute of Technology, Islampur-415414*

---

**Abstract -***The heat sink is the last and most influential part of the thermal stack, and is needed to first conduct heat away from the heat source and then to convect and radiate heat to the ambient. Micro channel provides the more surface area to volume ratio i.e. compactness, so it preferred in compact electronic devices as a heat sink. The plain Micro Channel Heat Sink (MCHS) is analyzed and validated with the published experimental data by comparing Nusselt number and Fanning friction factor at various inlet velocities ranging from 1.54 m/s to 6.17 m/s. In plain MCHS six different types of offset ribs are added on sidewall such as rectangular, backward triangular, forward triangular, mix of forward and backward triangular, isosceles and semicircular in shapes. All these geometries are analyzed at Reynolds number (Re) ranging from 200 to 800. The heat flux at the bottom of channel isgiven as $10^6$ W/$m^2$. Results shows that mix of forward and backward offset ribs MCHS gives better results as compared to other types of channel given conditions.*

***Key Words***: **Micro channel, Heat Sink, Numerical Simulation, Offset Ribs.**

## 1. INTRODUCTION

In today's technological world electronic components plays important role for different operations. During working of these electronic devices it generates heat, hence it is required to cool these components and maintain its temperature. This will increase its life and performance. The heat is carried away by using micro channel heat sink. As electronic devices are getting compact so it required compact cooling arrangement. Micro channel provides the less surface area to volume ratio i.e. more compactness, so it is preferred incompact electronic devices as a heat sink. Micro channel heat sink serves following objectives,

1. Very high surface area to volume ratio.
2. Large convective heat transfer coefficient.
3. It has small mass, small volume and small coolant inventory.
4. Bring fluid into intimate contact with the channel walls.
5. To bring fresh fluid to the walls and remove fluid away from the wall.
6. Experimental data showed that microchannel has a significant impact on the heat transfer rate for all fluid rates.
7. The unique construction of microchannel heat sink enables to bring heat source and heat sink into very close thermal proximity, thus minimizing thermal resistance.
8. It offers solutions to thermal dissipation problems for many existing and developing applications.

Chai L. et. al. [1] studied heat transfer enhancement in microchannel heat sinks with periodic expansion–constriction cross-sections. They investigated both experimental and numerical MCHS for fluid flow and heat transfer. Tukerman and Pease [2] first introduced the concept of MCHS in 1980s. Since this pioneering work, microchannel heat sinks have received considerable attention, and several studies have since been published which can be grouped as analytical, numerical or experimental.

Wang H et al. [3] studied the most common structure is a straight fin with a rectangular cross-section. Ma DD et al. [4] investigated how the microchannel structure plays a critical role in affecting the overall cooling capacity of the system. The simulation results showed that the microchannel cooler reduced the average die temperature and the staggered fins achieved better thermal performance than the straight fins. Wang KC et al. [5] investigated thermal performance of MCHS with triangular ribs in the transverse micro chambers. It shows that because of presence of ribs in transverse direction it create turbulence and which leads to the enhancement of heat transfer. Chai L. et al. [6] also investigated laminar flow and heat transfer characteristics of interrupted MCHS with ribs in the transverse micro chambers. Gong L. et al. [7] presented the numerical study on layout of MCHS for thermal management of electronic devices. Lu S. et al. [8] presented review on a comparative analysis of innovative MCHS for electronic cooling. They compared different MCHS by considering thermodynamic and geometrical parameters. Lei C. et al. [9] numerically investigated the characteristics of laminar flow and heat transfer in MCHS with offset ribs on sidewalls. Five different shapes are analyzed for different values of Re number.

## 2.NUMERICAL ANALYSIS of PLAIN MCHS

### 2.1CAD Model

Figure 1 shows CAD model drawn in Solid Works and Table 1 shows the dimensions used for modeling of the plain MCHS. All the dimensions of channel are less than 1 mm hence it is in the range of microchannel dimensions.

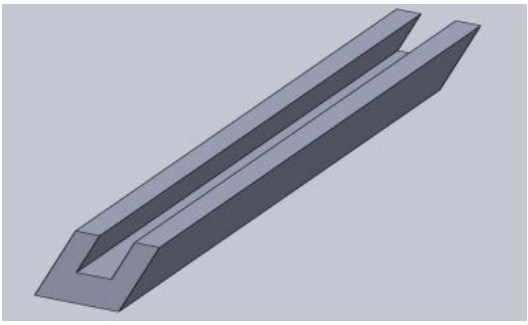

**Fig -1**: Modeling of plain MCHS

**Table -1:** Dimensions of plain MCHS

| Parameters | Computational Dimensions | Channel Dimensions |
|---|---|---|
| Length (mm) | 10 | 10 |
| Width (mm) | 0.25 | 0.1 |
| Height (mm) | 0.35 | 0.2 |

### 2.2 Meshing

Structured mesh is done with hexahedral components for plain MCHS. Figure 2 shows meshing view in three dimensions. Meshing details are like number of cells 25860, maximum skewness 0.52 and aspect ratio 2.7.

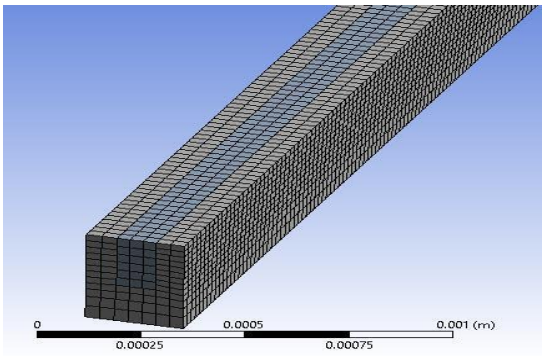


**Fig -2**: Meshing of pain MCHS

### 2.3Computational Method

Governing Equations

A three-dimensional, incompressible, steady state laminar flow model is designed. The conjugate effect of wall conduction and fluid axial conduction are important for simultaneously developing laminar flow and heat transfer in micro channels, thus the thermal conduction along flow direction and viscous dissipation are considered in this model. Figure 3 shows computational model of microchannel heat sink with offset ribs on sidewalls. The governing equations in the Cartesian tensor form are:

Continuity equation;

$$\frac{\partial u}{\partial x}+\frac{\partial v}{\partial y}+\frac{\partial w}{\partial z}=0 \quad (1)$$

Momentum Equations;

$$\rho\left(u\frac{\partial u}{\partial x}+v\frac{\partial u}{\partial y}+w\frac{\partial u}{\partial z}\right)=-\frac{\partial P}{\partial x}+\frac{\partial}{\partial x}\left(\mu\frac{\partial u}{\partial x}\right)+\frac{\partial}{\partial y}\left(\mu\frac{\partial u}{\partial y}\right)+\frac{\partial}{\partial z}\left(\mu\frac{\partial u}{\partial z}\right) \quad (2)$$

$$\rho\left(u\frac{\partial v}{\partial x}+v\frac{\partial v}{\partial y}+w\frac{\partial v}{\partial z}\right)=-\frac{\partial P}{\partial y}+\frac{\partial}{\partial x}\left(\mu\frac{\partial v}{\partial x}\right)+\frac{\partial}{\partial y}\left(\mu\frac{\partial v}{\partial y}\right)+\frac{\partial}{\partial z}\left(\mu\frac{\partial v}{\partial z}\right) \quad (3)$$

$$\rho\left(u\frac{\partial w}{\partial x}+v\frac{\partial w}{\partial y}+w\frac{\partial w}{\partial z}\right)=-\frac{\partial P}{\partial z}+\frac{\partial}{\partial x}\left(\mu\frac{\partial w}{\partial x}\right)+\frac{\partial}{\partial y}\left(\mu\frac{\partial w}{\partial y}\right)+\frac{\partial}{\partial z}\left(\mu\frac{\partial v}{\partial z}\right) \quad (4)$$

Energy Equation;

$$\rho C_p\left(u\frac{\partial T}{\partial x}+v\frac{\partial T}{\partial y}+w\frac{\partial T}{\partial z}\right)=\frac{\partial}{\partial x}\left(K\frac{\partial T}{\partial x}\right)+\frac{\partial}{\partial y}\left(K\frac{\partial T}{\partial y}\right)+\frac{\partial}{\partial z}\left(\mu\frac{\partial T}{\partial z}\right) \quad (5)$$

For the solid $\frac{\partial}{\partial X_i}\left(K_s\frac{\partial T}{\partial X_i}\right)=0$ (6)

Where,ρ is density, μis dynamic viscosity, $C_p$ is specific heat capacity, K is thermal conductivity.

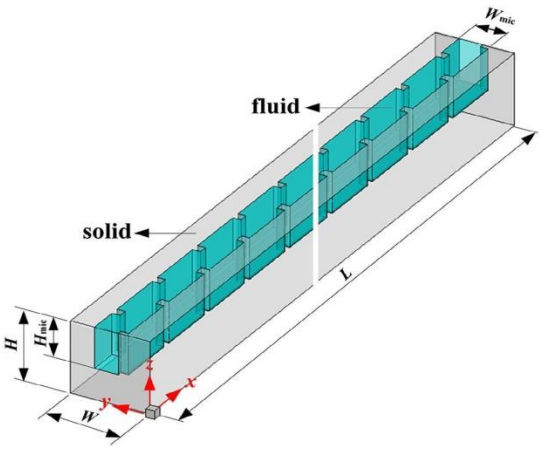


**Fig -3**: Computational model of microchannel heat sink with offset ribs on sidewalls

Computational Domain and Boundary Conditions

The fluid velocity at the microchannel inlet is assumed uniform

At x = o:

$u_f = u_{in}$ and $T_f = T_{in}$

Where, $u_{in}$ and $T_{in}$ are fluid velocity and temperature at the channel inlet. At the channel outlet, a pressure-outlet boundary condition is applied.

At x=L: $p_f = p_{out}$

where, $p_{out}$ is the given pressure.

For the inner wall/ fluid contact surface,

At u = v = w =0, $-k_s\frac{\partial T_s}{\partial n} = -k_f\frac{\partial T_f}{\partial n}$

where, n is the local coordinate normal to the wall. At the base of computational domain,

At z=0: $-k_s\frac{\partial T_s}{\partial z} = q_w$

At the two sides of the computational domain,

At y=0, $\frac{\partial T_s}{\partial y} = 0$

At y=w, $\frac{\partial T_s}{\partial y} = 0$

For other surfaces,

$$\frac{\partial T_f}{\partial x} = 0 \text{ or } \frac{\partial T_s}{\partial x} = 0$$

The parameters considered are in the following ranges: $u_{in}$= 1.54 – 6.17 m/s, $T_{in}$= 293 K, pout=0 (gauge pressure) and $q_w$= 106 W/m$^2$. The fluid and solid are water and silicon, respectively.

The thermal conductivity of silicon ks is set as a constant of 148 W/mK in the computations.

The length (L), width (W) and height (H) of the computational domain are 10 mm, 0.25 mm and 0.35 mm, respectively. The width ($W_{mic}$) and height ($H_{mic}$) in the microchannel region are 0.1 mm and 0.2 mm, respectively.

## 2.4Solution Methods and Convergence Criteria

The simulations are performed using the ANSYS FLUENT software. The SIMPLEC algorithm is applied to solve the governing differential equations for the velocity, pressure and temperature fields in the micro channels. For the micro channels with offset ribs on sidewalls, an unstructured mesh based on rectangular grid elements is utilized. A non-uniform arrangement with a large number of grids is arranged near the offset ribs. The solutions are considered to be converged when the normalized residual values are less than 10-5 for all the variables.

## 2.5Data Acquisition

Parameters characterizing the fluid flow and heat transfer in the micro channels are of interest in the present work. The Reynolds number is defined as

$$Re = \frac{\rho_f u_m D_h}{\mu_f} \quad (7)$$

Where,$\rho_f$ is the volume-average fluid density, $u_m$ is the average flow velocity in the smooth channel section, $D_h$ is the hydraulic diameter calculated based on the channel section without offset ribs, $D_h$is the mass-average fluid dynamic viscosity.

The average Fanning friction factor is given by

$$f = \frac{\Delta p\, D_h}{2\rho_f L u_m^2} \quad (8)$$

The average heat transfer coefficient and Nusselt number are given by

$$h = \frac{q_w A_w}{A_{con}(T_w - T_f)} \quad (9)$$

$$Nu = \frac{hD_h}{k_f} \quad (10)$$

Where, Aw is the silicon base area, Acon is the inner wall or fluid contact surface area, kf is the mass-average fluid thermal conductivity, Tw is the area-weighted temperature of the silicon base, Tf is the mass-average temperature of water in microchannel.

## 2.6 Validation for Smooth Microchannel Heat Sink

A validation of plain microchannel heat sink is performed by comparing with the experimental data of Chai et al. [1] and theoretical data obtained by 16/Re formulae. Figure 4 shows comparison of numerical results of Nu vs Re with experimental data of smooth MCHS. Figure 5 shows comparison of numerical results of fe vs Re with experimental data for smooth MCHS. It shows that numerical results of Nusselt number and friction factor for different Reynolds number are in good agreement with published experimental data.

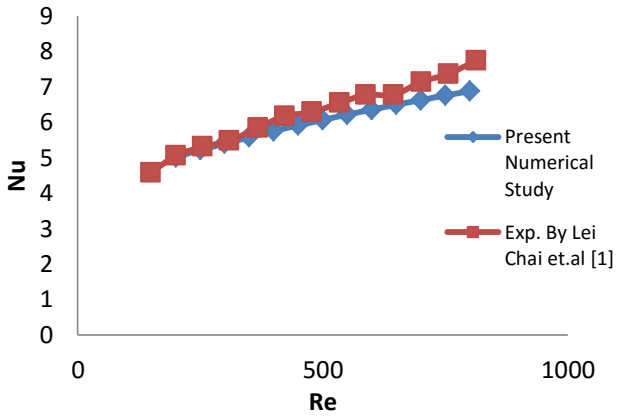


**Fig -4**: Comparison of numerical results of Nu vs Re with experimental data for the smooth MCHS

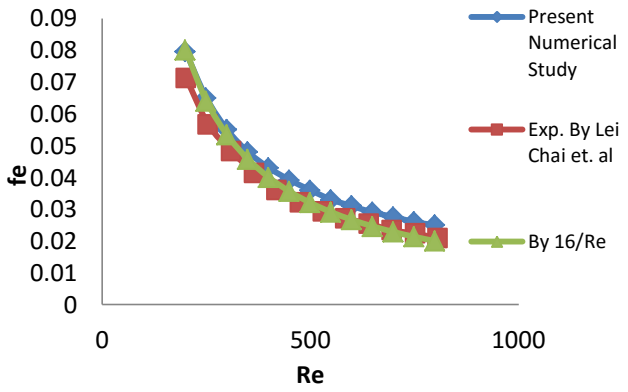


**Fig -5**: Comparison of numerical results of fe vs Re with experimental data for the smooth MCHS

## 3. RESULTS AND DISCUSSION

Figure 6 shows temperature distribution on the bottom face of MCHS. It is seen that low temperature is on inlet side and it goes on increasing towards outlet of channel. Figure 7 shows pressure distribution in the flow domain of channel. The high pressure is on inlet side and it goes on decreasing towards outlet.

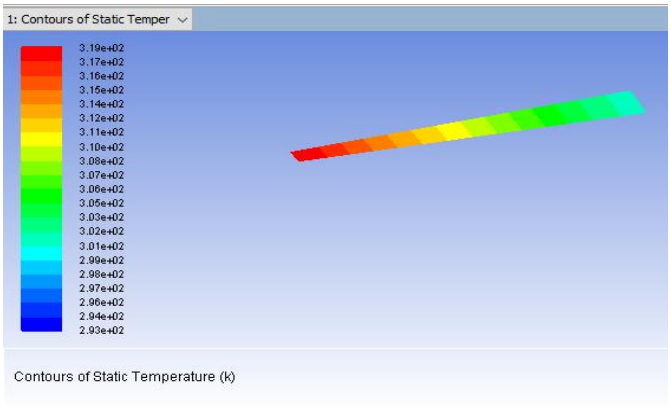


**Fig -6**: Temperature at bottom face for plain MCHS

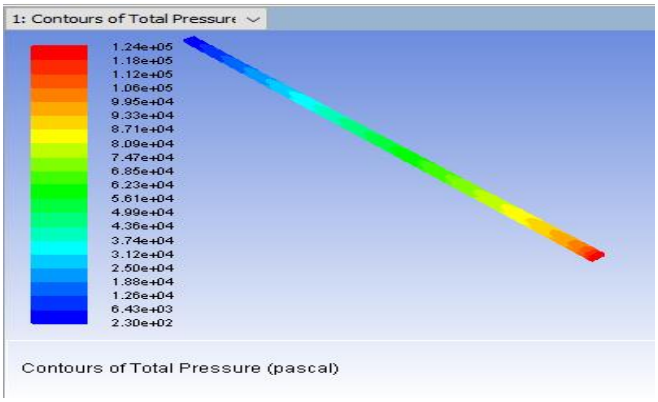


**Fig -7**: Contours of pressure in flow domain of MCHS

## 4. NUMERICAL SIMULATION of MCHS WITH OFFSET RIBS

### 4.1 Modification in Geometries

In plain MCHS offset ribs are added to create turbulence and thereby increase in heat transfer rate. Total 25 offset ribs are added on each side of microchannel on equal distances. Because of offset ribs turbulence will create near to the wall and it will redevelop boundary layer and new fluid will come in contact with wall thereby increase in convection heat transfer rate.

### 4.2 CAD Models of all Modified Geometries

A MCHS with offset ribs are modeled in Solid Works. Figure 8 shows six types of offset ribs such as rectangular, backward triangular, forward triangular, mix of forward and backward triangular, isosceles and semicircular ribs. The length, width and height of ribs are 0.05,0.025 and 0.2 mm respectively. The distance between two ribs is 0.4 mm and total 25 ribs are added on both sides of microchannel [9].

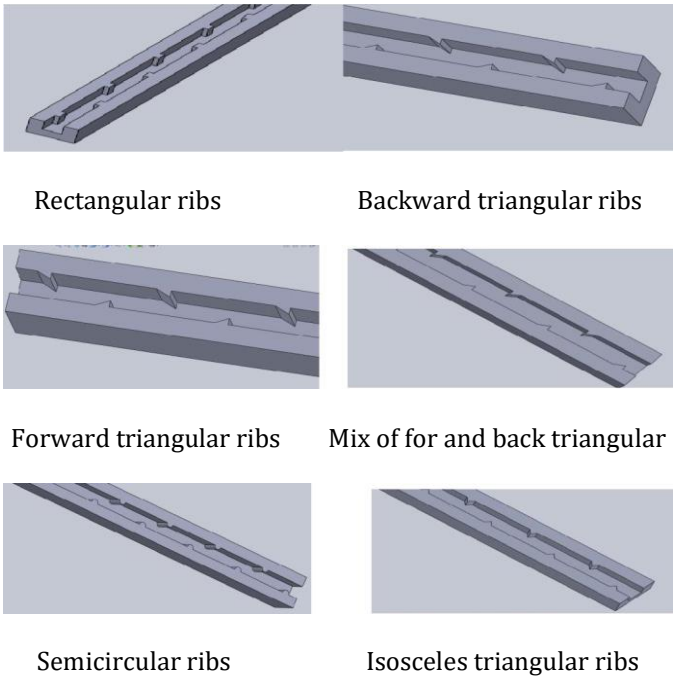


**Fig -8**: CAD models of different types of offset ribs MCHS

### 4.3 Meshing

Meshing of CAD model is done in ANSYS mesh by finite volume method. Tetrahedron unstructured mesh is done to all the CAD models. Fine mesh is created near to the ribs toimprove the meshing as there is creation of little turbulence in that region. Figure 9 shows meshing of all types of offset ribs MCHS.

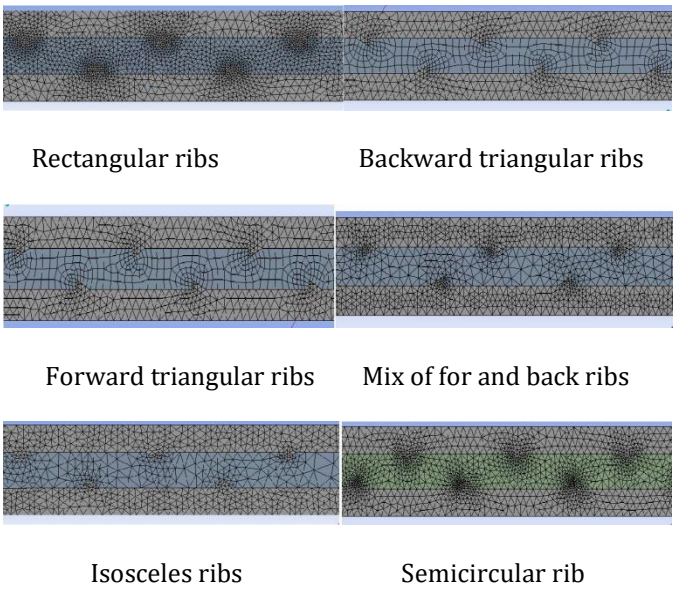


**Fig -9**: Meshing of different types of offset ribs of MCHS in x-y plane (z=0.25 mm)

### 4.4 Temperature and Pressure Contours

Figure 10 shows temperature contour at Re 500 and fluid inlet velocity of 3.86 m/s for mix of forward and backward offset ribs MCHS. The temperature contour shows low temperature on inlet side and it goes on increasing towards outlet. Figure 11 shows pressure contour at Re 500 and fluid inlet velocity of 3.86 m/s. In pressure contour high pressure is at inlet side and it goes on decreasing towards outlet.

### 4.5 Heat Transfer

Figure 12 shows variation of Nu with Re for different channels. The rise in Nu is rapid up to Re 500 and after that rate of increases of Nu number decreases slowly. Results of heat transfer shows that out of all modified MCHS mix of forward and backward triangular ribs MCHS gives better results.

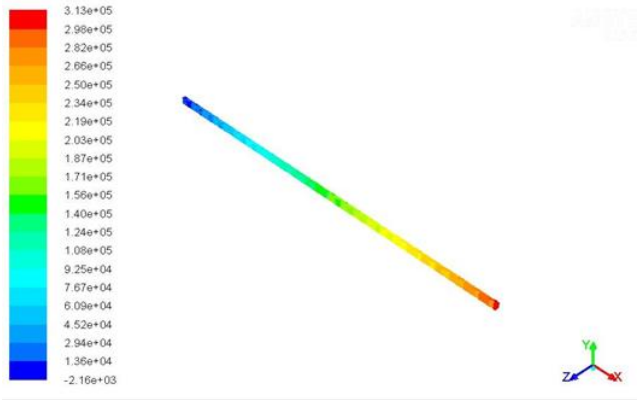


**Fig -10**: Temperature contour of MCHS with mix of forward and backward offset ribs

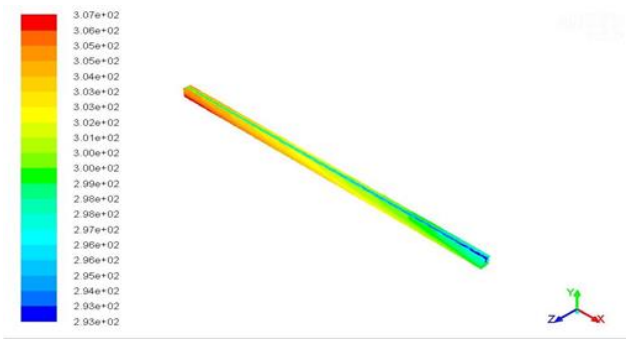


**Fig -11**: Pressure contour of MCHS with mix of forward and backward offset ribs

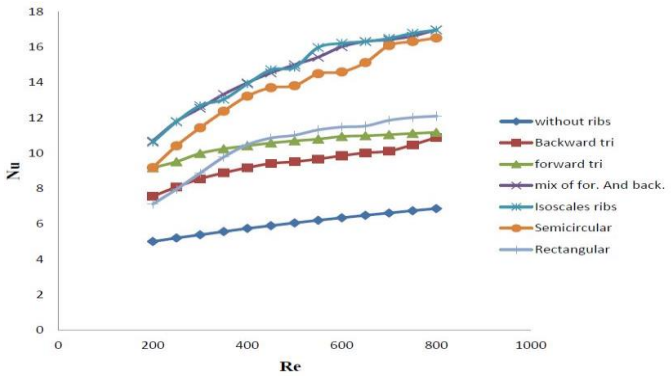


**Fig -12**: Variation of Nu with Re for different channels

### 4.6 Pressure Drop

Figure 13 shows variation of ΔP with Re for different channels. In this pressure drop is estimated for various Re number ranging from 200 to 800. It is seen that as Re increases there is increase in pressure drop. In case of forward triangular ribs MCHS there is less pressure drop as compared to other types of channels with highest heat transfer rate, so this geometry is selected as best geometry among all types of modified MCHS. In case of isosceles triangular ribs rate of pressure drop is more after Re 600. Forward triangular ribs MCHS gives lowest pressure drop as compared to other types of MCHS, but it also gives lowest heat transfer rate, so it is not selected as best geometry.

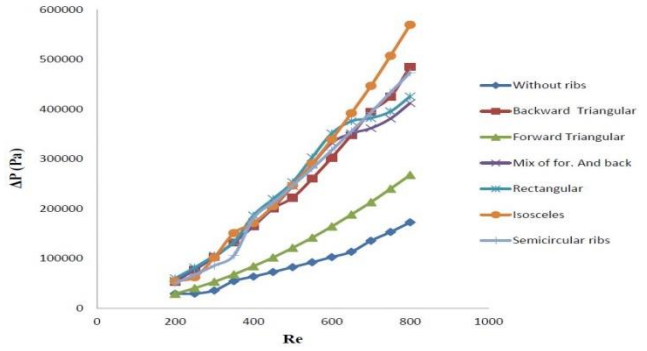


**Fig -13**: Variation of ΔP with Re for different channels

### 4.7 Temperature Distribution

Figure 14 shows variation of $T_b$ with Re for different channels. Temperature distribution at bottom face of MCHS is calculated for different types of channels at various Reynolds number ranging from 200 to 800. In case of plain MCHS temperature at bottom face is 323.4 K to 312.82 K at various Reynolds number ranging from 200 to 800. By adding offset ribs in plain MCHS there is creation of turbulence which leads to the increase in heat transfer rate from MCHS to the fluid and thereby decrease in the bottom face temperature. For various MCHS with different offset ribs at Re 500, mix of forward and backward MCHS gives lowest temperature which is 304.25 K.

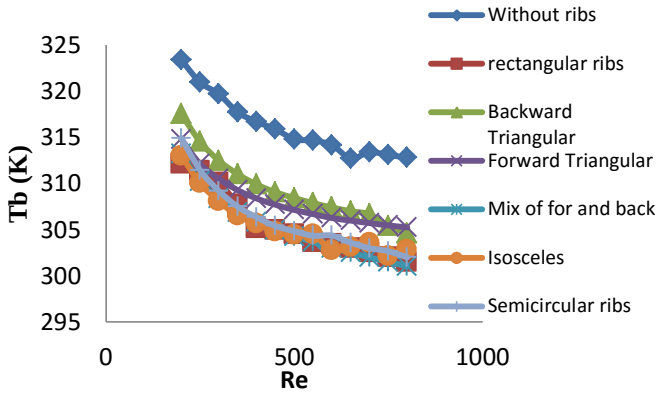


**Fig -14**: Variation of $T_b$ with Re for different channels

### 4.8 Selection MCHS with Offset Ribs

After simulation of all types of MCHS based on different thermal parameters best geometry is selected. Results shows that mix of forward and backward offset ribs type MCHS gives least temperature at the bottom face with permissible pressure drop as compared to other types of MCHS. Table 2 shows values of different thermal parameters at Re 500 and heatflux 106 W/cm2.

**Table -2:** Comparison of thermal parameters for different types of modified MCHS at Re 500 and heat flux 100 W/cm$^2$

| Types of offset ribs | Nu | ΔP (Kpa) | $T_b$ |
|---|---|---|---|
| Without ribs | 6.06 | 82.336 | 314.82 |
| Rectangular ribs | 11.02 | 253.253 | 304.48 |
| Forward triangular | 10.7 | 121.157 | 307.15 |
| Backward triangular | 9.52 | 221.995 | 308.45 |
| **Mix of forward and backward triangular** | **15.01** | **245.738** | **304.25** |
| Isosceles ribs | 14.58 | 246.486 | 304.44 |
| Semicircular ribs | 13.82 | 246.539 | 304.84 |

## 5. CONCLUSION

This paper presents numerical analysis plain and offset ribs MCHS. The 3D analysis with conjugate heat transfer and viscous heating is presented for fluid flow and heat transfer in MCHS. Results show that with increase in Re the Nu increases and friction factor decreases for selected MCHS. The trade-off is required between Nu and pressure drop for given operating conditions of MCHS.

1. For plain MCHS at Re 500 and heat flux 106 W/m2 gives Nu 6.06, P 82.33KPa, and Tb 314.82 K.

2. For mix of forward and backward triangular offset ribs MCHS at Re 500 and heat flux 106 W/m2 it gives Nu 15.01, P 245 KPa and Tb 304.25 K.

3. Result with mix of forward and backward triangular offset ribs MCHS shows minimum 53% to maximum 60% increase in Nu number for Re between 200 to 800 respectively as compared to plain MCHS

4. The mix of forward and backward triangular offset ribs MCHS shows better results at selected operating conditions.

## REFERENCES

[1]Chai L., Xia G., Wang L., Zhou M. and Cui Z., "Heat transfer enhancement in microchannel heat sinks with periodic expansion–constriction cross-sections," InternationalJournal of Heat and Mass Transfer, vol.31;62, 2013, 741-51.

[2] D.B. Tuckerman and R.F.W. Pease, "High-performance heat sinking for VLSI,"Electron.Dev. Lett., 1981,126–129.

[3] Wang H., Chen Z. and Gao J., "Influence of geometric parameters on flow and heat transfer performance of micro-channel heat sinks," Applied Thermal Engineering, vol.25;107, 2016, 870-9.

[4] Ma DD., Xia GD., Li YF., Jia YT. and Wang J., "Effects of structural parameters on fluid flow and heat transfer characteristics in microchannel with offset zigzag grooves in sidewall," International Journal of Heat and Mass Transfer, vol.31;101, 2016, 427-35.

[5] Wong KC. and Lee JH., "Investigation of thermal performance of microchannel heat sink with triangular ribs in the transverse microchambers," International Communications inHeat and Mass Transfer, vol.31;65, 2015, 103-10.

[6] Chai L., Xia GD. and Wang HS., "Laminar flow and heat transfer characteristics of interrupted microchannel heat sink with ribs in the transverse microchambers,"International Journal of Thermal Sciences, vol.31;110, 2016, 1-1.

[7] Gong L., Zhao J. and Huang S., "Numerical study on layout of micro-channel heat sink for thermal management of electronic devices," Applied Thermal Engineering, vol.5;88, 2015, 480-90.

[8] Lu S. andVafai K., "A comparative analysis of innovative microchannel heat sinks for electronic cooling," International Communications in Heat and Mass Transfer, vol.31;76, 2016, 271-84.

[9] Lei C., Guo D. and Hua S., "Numerical study of laminar flow and heat transfer in microchannel heat sink with offset ribs on sidewalls," Applied Thermal Engineering, 2016, 32–41.